Liquid Crystals

ISSN: 0267-8292 (Print) 1366-5855 (Online) Journal homepage: http://www.tandfonline.com/loi/tlct20

New isothiocyanatotolane liquid crystals with terminal but-3-enyl substitute

Juanli Li, Jian Li, Minggang Hu, Zhongwei An, Zenghui Peng, Lu Zhang & Ning Gan

To cite this article: Juanli Li, Jian Li, Minggang Hu, Zhongwei An, Zenghui Peng, Lu Zhang & Ning Gan (2017) New isothiocyanatotolane liquid crystals with terminal but-3-enyl substitute, Liquid Crystals, 44:5, 833-842, DOI: 10.1080/02678292.2016.1247478

To link to this article: https://doi.org/10.1080/02678292.2016.1247478

LIQUID CRYSTALS, 2017
VOL. 44, NO. 5, 833–842
https://doi.org/10.1080/02678292.2016.1247478

Taylor & Francis
Taylor & Francis Group

New isothiocyanatotolane liquid crystals with terminal but-3-enyl substitute

Juanli Li[a,b], Jian Li[a,b], Minggang Hu[a,b], Zhongwei An[a,b,c], Zenghui Peng[d], Lu Zhang[a,b] and Ning Gan[a,b]

[a]State Key Laboratory of Fluorine & Nitrogen Chemicals, Xi'an, P. R. China; [b]Optical and Electrical Material Center, Xi'an Modern Chemistry Research Institute, Xi'an, P. R. China; [c]School of Materials Science and Engineering, Shaanxi Normal University, Xi'an, P. R. China; [d]State Key Laboratory of Applied Optics, Changchun Institute of Optics, Fine Mechanics and Physics, Chinese Academy of Sciences, Changchun, P. R. China

ABSTRACT

Four kinds of new but-3-enyl-based isothiocyanate liquid crystals composed of tolane core and but-3-enyl terminal group (**A1**–**A4**) were synthesised via seven step reactions based on 2-(4-bromophenethyl)-1,3-dioxolane, and four *n*-butyl analogues **B1**–**B4** as comparison structures were also prepared. The mesomorphic properties and physical properties of the compounds were investigated. Single fluorinated compounds **A2** and **A3** exhibit monotropic nematic phase, and they have lower melting enthalpy and higher clearing points than those of the comparison compounds **B2** and **B3**. The non-fluoro-substituted compound **A1** and difluorinated compound **A4** exhibit no nematic phase. Replacement of *n*-butyl chain by but-3-enyl as terminal group is enabled to increase birefringence (Δn ~ 0.394–0.430) and reduce rotational viscosity. These isothiocyanatotolanes with terminal but-3-enyl substitution have potential application for high birefringence mixtures.

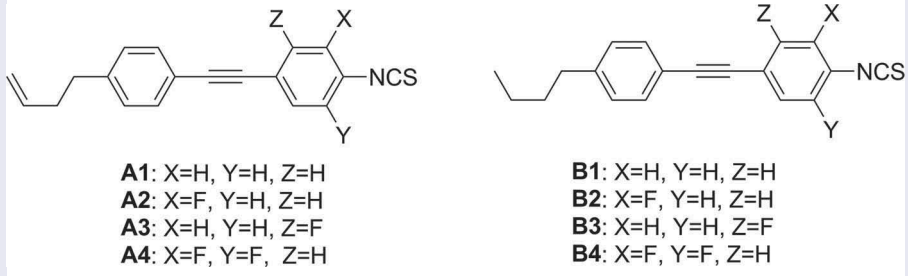

A1: X=H, Y=H, Z=H
A2: X=F, Y=H, Z=H
A3: X=H, Y=H, Z=F
A4: X=F, Y=F, Z=H

B1: X=H, Y=H, Z=H
B2: X=F, Y=H, Z=H
B3: X=H, Y=H, Z=F
B4: X=F, Y=F, Z=H

1. Target compounds **A** and the comparison structures **B**.

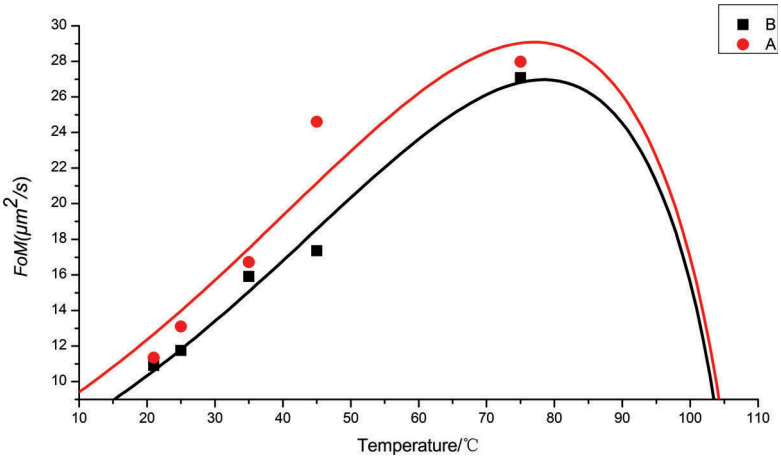

2. Mixture **A** based compounds **A1** and **A2** exhibits higher value of FoM than Mix **B** based compounds **B1** and **B2**.

ARTICLE HISTORY
Received 18 July 2016
Accepted 9 October 2016

KEYWORDS
Isothiocyanate; monotropic nematic phase; birefringence; rotational viscosity

CONTACT Zhongwei An gmecazw@163.com State Key Laboratory of Fluorine & Nitrogen Chemicals, Xi'an, P. R. China; Xi'an Modern Chemistry Research Institute, Xi'an, P. R. China; School of Materials Science and Engineering, Shaanxi Normal University, Xi'an, P. R. China

Supplemental data for this article can be accessed here.

1. Introduction

Liquid crystal materials (LCs) with high birefringence are very popular with the development of the new photonic devices, such as tunable spatial modulators for light [1,2] and laser beam steering [3], and tunable focus lenses [4,5], and so on. More recently, high birefringence LCs have also earned growing interest as base materials for devices in the GHz and THz regions [6,7].

Almost all LC-related devices require faster response times. In order to achieve this purpose, the straight forward approach is applied to use a thin cell gap filled with a high birefringence and low viscosity LC materials. LC compounds with tolane core exhibit reasonably high values of Δn, low viscosity, and good chemical, photo as well as thermal stability [8]. Isothiocyanates deliver the same properties as tolanes [9]. Therefore, combination of the tolane with NCS group leads to high optical anisotropy meanwhile maintaining a relatively low viscosity, for example, the compound B2 in Figure 1 as a typical high birefringence structure exhibits Δn value of 0.364 [10].

During the last decades, plenty of studies have focused on the LC compounds and mixtures-based isothiocyanatotolanes with saturated alkyl chain as terminal group [11–15], and only few of them on terminal alkenyl-substituted isothiocyanatotolane structures have been reported [16]. It is noted that series of unsaturated alkenyl groups, ethenyl, allyl and but-3-enyl, have also been reported to serve as terminal chain to improve the elastic constant ratio, mesophase range of fluorinated LCs [17–20]. With the aim to increase the birefringence and lower the rotational viscosity of isothiocyanatotolanes and to search for new LCs for high birefringence mixtures, we have designed and prepared four but-3-enyl-based isothiocyanatotolanes **A1**–**A4** (see Figure 1) with birefringence (~0.394–0.43) and low rotational viscosity. Their thermal properties and the mixtures based on these compounds are also presented. The reference compounds **B1**–**B4** were synthesised by using the method reported in [12].

2. Experiment

2.1. Materials

2-(4-Bromophenethy)-1,3-dioxolane and methyltriphenylphosphornium bromide were purchased from Xi'an Caijing Opto-Electrical Science Technology Co. Ltd. Ethynyltrimethylsilane was purchased from Shanghai Bangcheng Chemical Co. Ltd. 4-Iodoaniline and 2-fluoro-4-iodoaniline were purchased from Shanghai Zhuorui Chemical Co. Ltd. Potassium *tert*-butoxide, copper(I)iodide, dichlorois(triphenylphosphine)palladium, potassium hydroxide, calcium carbonate, triphenylphosphine, chloroform and thiophosgene were purchased from TCI Chemical Reagent Co.

2.2. Characterization

The structures of the final products were confirmed by a variety of spectral methods. ^{1}H-nuclear magnetic resonance (^{1}H NMR) with tetramethylsilane as internal standard was recorded on a Bruker AV500 (500 MHz) instrument. IR spectra were recorded using a Nicolet Avatar360E spectrometer. The mass spectra (MS) were obtained by GC/MS Thermo DSQ with m/z 50–650. The phase transitions of the final products were determined using a Mettle HS82 heating stage and HS1 temperature control unit in conjunction with a Nikon polarising optical microscopy, and the transition temperatures were confirmed by DSC analysis (TA-Q20) in nitrogen at heating and cooling rate of 5°C/min.

The physical properties of the single compound were obtained from 10 wt% solutions in the host mixture P0 (with melting point of 6°C, clearing point of 112.7°C) [21] by extrapolation. The rotational viscosity of the LC compounds was measured by IV1-Cust (Instec) in a homogeneous cell with cell gap

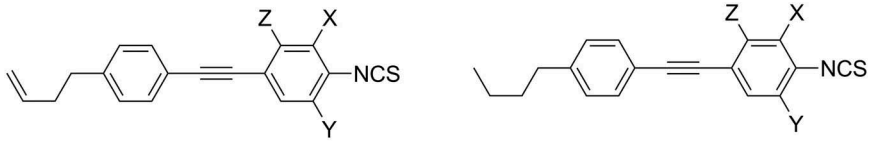

A1: X=H, Y=H, Z=H
A2: X=F, Y=H, Z=H
A3: X=H, Y=H, Z=F
A4: X=F, Y=F, Z=H

B1: X=H, Y=H, Z=H
B2: X=F, Y=H, Z=H
B3: X=H, Y=H, Z=F
B4: X=F, Y=F, Z=H

Figure 1. Target compounds and the comparison structures.

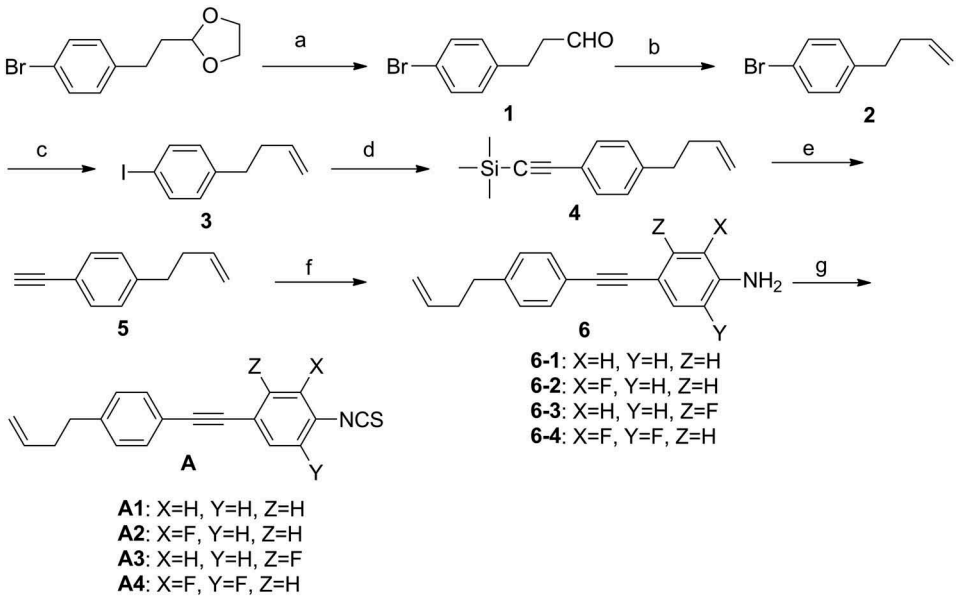

Scheme 1. Synthetic route of compounds **A1**–**A4**. (a) HCOOH, toluene. (b) $CH_3P^+Ph_3Br^-$, t-$(CH_3)_3COK$, THF. (c) *n*-BuLi, I_2, THF. (d) 1. Pd$(PPh_3)_2Cl_2$, CuI, PPh_3, Et_3 N, TMSA; 2. KOH, EtOH. (e) 4-iodoaniline, 2-fluorine-4-iodoaniline, 3-fluorine-4-iodoaniline or 2,6-difluorine-4-iodoaniline, Pd$(PPh_3)_2Cl_2$, CuI, PPh_3, Et_3 N. (f) $CSCl_2$, $CaCO_3$, $CHCl_3$, H_2O.

$d \approx 10$ μm. The response time was measured by IV1-Cust (Instec) in a 90° twist cell with cell gap $d \approx 5$ μm. The birefringence was measured using an Abbe refractometer (λ = 589 nm). All of the measurements were carried out at 25°C.

2.3. Synthesis

The new but-3-enyl-based isothiocyanatotolane compounds **A1**–**A4** were prepared using the route shown in Scheme 1.

2.3.1. Synthesis of 3-(4-bromophenyl)propanal (1)

A mixture of 2-(4-bromophenethyl)-1,3-dioxolane (51.4 g, 0.2 mol), formic acid (102.8 g, 0.4 mol) and toluene (150 mL) was heated at reflux for 1 h. After cooling the mixture to room temperature, the organic layer was separated and mixed again with formic acid (102.8 g, 0.4 mol). The above actions were repeated three times, then the organic layer was separated, washed with water and dried over anhydrous $MgSO_4$. The product was isolated by evaporating the solvent to give a yellow liquid with a yield of 89% and GC purity of 95.42%. ^{1}H NMR ($CDCl_3$, 500 MHz) δ (ppm): 2.747–2.780 (m, 2*H*), 2.893–2.923 (t, 2*H*), 7.055–7.082 (m, 2*H*), 7.393–7.420 (m, 2*H*), 9.802–9.807 (t, 1*H*); IR(KBr, cm^{-1}): 3026, 2928, 2725, 1723, 1489, 1447, 1405, 828, 712, 693; MS *m*/*z* (relative intensity [RI], %): 212.1 (M^+, 89), 214.0 (M^+ + 2, 88), 171.0, 169.0 (100), 156, 158 (29), 133.1 (80), 104.1 (39), 91.1 (48), 77.0 (32).

2.3.2. Synthesis of 1-bromo-4-(but-3-enyl)benzene (2)

A solution of $CH_3P^+Ph_3Br^-$ (91.5 g, 0.256 mol) dissolved in THF (100 mL) was stirred at −10–0°C under nitrogen. Then potassium *tert*-butoxide was added and the solution was stirred 1 h. A solution of 3-(4-bromophenyl)propanal (39 g, 0.183 mol) dissolved in THF (200 mL) was dropped with stirring for about 3 h at −10–0°C and allowed to warm to room temperature, then water (100 mL) and *n*-heptane (200 mL) were added and the mixture stirred 30 min. The organic layer was separated and the aqueous layer was extracted with *n*-heptane. The combined organic layers were dried over anhydrous $MgSO_4$. The crude product was isolated by evaporating the solvent, and purified by column chromatography using *n*-heptane as eluent to give a yellow liquid. The yellow liquid was distiled under reduced pressure, and the fraction of 1-bromo-4-(but-3-enyl)benzene was collected at 74–80°C/60 Pa with a yield of 81% and GC purity of 99.35%. ^{1}H NMR ($CDCl_3$, 500 MHz) δ (ppm): 2.309–2.358 (m, 2*H*), 2.633–2.664 (t, 2*H*), 4.959–5.040 (m, 2*H*), 5.769–5.850 (m, 1*H*), 7.027–7.054 (m, 2*H*), 7.366–7.393 (m, 2*H*); IR (KBr, cm^{-1}): 3078, 3039, 3024, 2999, 2930, 2857, 1592, 1488, 1452, 1440, 1403, 995, 913, 840, 827, 771, 602; MS *m*/*z* (RI, %): 210.0 (M^+, 13), 212.0 (M^+ + 2, 13), 171.0, 169.0 (100), 133.0 (13), 90.0 (16), 89.0 (11).

2.3.3. Synthesis of 1-(but-3-enyl)-4-iodobenzene (3)

Under nitrogen protection, 2.4 M butyl lithium (94 mL, 0.224 mol) was injected into a cooled (−78°

C), stirred solution of 1-bromo-4-(but-3-enyl)benzene (43 g, 0.204 mol) in THF (200 mL). After addition, the reaction temperature was maintained at −78°C for 2 h, followed by the addition of iodine (57 g, 0.224 mol) in THF (80 mL) and allowed to warm to room temperature overnight. $NaHSO_3$ (20 g) solved in water (400 mL) was added, *n*-heptane was added for three extraction cycles. The combined organic extracts were washed with water (400 mL), dried over anhydrous $MgSO_4$. The crude product was isolated by evaporating the solvent, and purified by distiling under reduced pressure, and the fraction of 1-(but-3-enyl)-4-iodobenzene was collected at 80–88°C/60 Pa with a yield of 84% and GC purity of 97.35%. ^{1}H NMR ($CDCl_3$, 500 MHz) δ (ppm): 2.314–2.364 (m, 2*H*), 2.634–2.666 (t, 2*H*), 4.964–5.045 (m, 2*H*), 5.775–5.856 (m, 1*H*), 6.928–6.944 (d, J = 8 Hz, 2*H*), 7.577–7.603 (m, 2*H*); IR (KBr, cm^{-1}): 3076, 3015, 3001, 2977, 2928, 2855, 1588, 1484, 1439, 1415, 1399, 913, 824, 805, 767; MS *m*/*z* (RI, %): 258.1 (M^+, 25), 217.1 (100), 131.1 (8), 90.1 (18), 63.1 (2).

2.3.4. Synthesis of ((4-(but-3-en-1-yl)phenyl)ethynyl) trimethylsilane (4)

Ethynyltrimethylsilane (18 g, 0.18 mol) in dry triethylamine was added dropwise to a suspension of 1-(but-3-enyl)-4-iodobenzene (44 g, 0.171 mol), $Pd(PPh_3)_2Cl_2$ (1.2 g, 1.71 mmol), copper(I)iodide (0.98 g, 5.13 mmol) and triphenylphosphine (1.34 g, 5.13 mmol) in dry triethylamine (100 mL) at room temperature. The solution was heated at 40°C and stirred for 2 h. The mixture was then cooled and filtered, and the solvents were evaporated, *n*-heptane was added and the organic layer was washed with saturated ammonium chloride solution, dried over anhydrous $MgSO_4$ and the solvents were evaporated. The crude product was purified by column chromatography using *n*-heptane as eluent, to give a yellow liquid, yield 98% with GC purity of 90.54%. MS *m*/*z* (RI, %): 228.1 (M^+, 30), 213.1 (54), 187.1 (100), 172.0 (30), 159.0 (30), 105.0 (3).

2.3.5. Synthesis of 1-(but-3-enyl)-4-ethynylbenzene (5)

A mixture of compound 4 (38.7 g, 0.17 mol) and potassium hydroxide (9.5 g, 0.17 mol) in ethanol (430 mL) was stirred at room temperature for 1 h. Then *n*-heptane was added and the organic layer was washed with water, dried over anhydrous $MgSO_4$ and the solvents were evaporated. A red liquid was given, yield 89% with GC purity of 98.12%. ^{1}H NMR ($CDCl_3$, 500 MHz) δ (ppm): 2.334–2.383 (m, 2*H*), 2.691–2.722 (t, 2*H*), 3.032 (s, 1*H*), 4.964–5.050 (m, 2*H*), 5.786–5.887 (m, 1*H*), 7.131–7.148 (d, J = 8.5 Hz, 2*H*), 7.402–7.418 (q, 2*H*); IR (KBr, cm^{-1}): 3295, 3079, 3029, 2929, 2857, 2108, 1640, 1508, 1440, 1412, 914, 839; MS *m*/*z* (RI, %): 156.1 (M^+, 27), 115.1 (100), 89.1 (10), 63.0 (6).

2.3.6. Synthesis of 4-((4-(but-3-enyl)phenyl)ethynyl) aniline (6-1)

2-Fluoro-4-iodoaniline (3.7 g, 17 mmol), $Pd(PPh_3)_2Cl_2$ (0.12 g, 0.19 mmol), triphenylphosphine (0.13 g, 0.57 mmol), copper(I)iodide (0.1 g, 0.57 mmol) and dry triethylamine (50 mL) were mixed and stirred at room temperature under nitrogen. A solution of compound 5 (2.96 g, 19 mmol) dissolved in 10 mL of dry triethylamine was added dropwise and the mixture stirred at 30°C for 2 h. The mixture was filtered and the filtrate was concentrated in vacuum to remove triethylamine. The crude product was dissolved in toluene and extracted with toluene. The organic layer was then washed with saturated ammonium chloride and dried over anhydrous $MgSO_4$. After removal of the solvent in vacuum, the residue was recrystallised two times from the mixing solution of *n*-heptane (20 mL) and toluene (2 mL) at −20°C to obtain 4-((4-(but-3-enyl)phenyl)ethynyl)aniline as yellow crystals, yield 82% with GC purity of 98.30%. M.p.: 67.23–68.73°C; ^{1}H NMR ($CDCl_3$, 500 MHz) δ (ppm): 2.343–2.387 (q, 2*H*), 2.688–2.720 (t, 2*H*), 3.793 (s, 2*H*), 4.968–5.050 (m, 2*H*), 5.798–5.879 (m, 1*H*), 6.615–6.632 (d, J = 8.5 Hz, 2*H*), 7.130–7.146 (d, J = 8 Hz, 2*H*), 7.314–7.331 (d, J = 8.5 Hz, 2*H*), 7.399–7.415 (d, J = 8 Hz, 2*H*); IR (KBr, cm^{-1}): 3469, 3377, 3076, 3030, 2976, 2922, 2852, 2206, 1639, 1617, 1598, 1452, 1432, 1410, 993, 991, 827; MS *m*/*z* (RI, %): 247.0 (M^+, 37), 206.0 (100), 178.0 (5), 152.0 (2).

6-2: The yield of 50% with GC purity of 97.40%, yellow crystals. M.p.: 66.02–67.40°C; ^{1}H NMR ($CDCl_3$, 500 MHz) δ (ppm): 2.380–2.425 (q, 2*H*), 2.729–2.760 (t, 2*H*), 3.885 (s, 2*H*), 5.004–5.090 (m, 2*H*), 5.832–5.913 (m, 1*H*), 6.727–6.762 (t, 1*H*), 7.144–7.204 (m, 4*H*), 7.434–7.450 (d, J = 8 Hz, 2*H*); IR (KBr, cm^{-1}): 3481, 3390, 3068, 3026, 2974, 2855, 2209, 1632, 1571, 1520, 1435, 1193, 1106, 947, 860; MS *m*/*z* (RI, %): 265.0 (M^+, 44), 224.0 (100), 206.9 (3), 176.0 (4).

6-3: The yield of 77% with GC purity of 98.25%, yellow crystals. M.p.: 41.48–42.41; ^{1}H NMR ($CDCl_3$, 500 MHz) δ (ppm): 2.344–2.388 (q, 2*H*), 2.693–2.724 (t, 2*H*), 3.906 (s, 2*H*), 4.966–5.053 (m, 2*H*), 5.797–5.878 (m, 1*H*), 6.372–6.410(m, 2*H*), 7.138–7.154 (d, J = 8 Hz, 2*H*), 7.256–7.282 (m, 1*H*), 7.422–7.439 (d, J = 8.5 Hz, 2*H*); IR (KBr, cm^{-1}): 3443, 3421, 3078, 3028, 2921, 2852, 2213, 1621, 1563, 1521, 1452, 1167, 1114, 960, 841; MS *m*/*z* (RI, %): 265.1 (M^+, 43), 224.1 (100), 196.0 (5), 176.0 (3).

6-4: The yield of 60% with GC purity of 98.01%, brown crystals. M.p.: 59.44–61.60°C; ^{1}H NMR ($CDCl_3$,

500 MHz) δ (ppm): 2.345–2.391 (m, 2*H*), 2.699–2.730 (t, 2*H*), 3.872 (s, 2*H*), 4.967–5.054 (m, 2*H*), 5.796–5.877 (m, 1*H*), 6.960–7.030 (m, 2*H*), 7.146–7.163 (d, J = 8.5 Hz, 2*H*), 7.394–7.410 (d, J = 8Hz, 2H); IR (KBr, cm^{-1}): 3421, 3312, 3083, 2929, 2852, 2201, 1640, 1452, 1434, 918, 826; MS *m*/*z* (RI, %): 283.0 (M^+, 41), 242.1 (100), 221.0 (3), 194.0 (4).

2.3.7. Synthesis of 1-(but-3-enyl)-4-((4-isothiocyanatophenyl)ethynyl)benzene (A1)

A solution of the prepared compound 6-1 (1.2 g, 4.84 mmol) dissolved in $CHCl_3$ (40 mL) was added dropwise to a stirred mixture of $CHCl_3$ (20 mL), water (20 mL), $CaCO_3$ (2.42 g, 24.2 mmol) and thiophosgene (0.9 g, 7.26 mmol) at −5°C. The mixture was stirred for 1 h at room temperature and then heated to reflux for 2 h; it was then filtered and the organic layer separated and dried over anhydrous $MgSO_4$. After removal of the solvent, the crude product was dissolved in *n*-heptane and eluted two times at room temperature on a chromatographic column filled with silica gel by using *n*-heptane as eluent. The colourless eluent was concentrated to dryness and the solid was crystallised at −20°C from acetone (20 mL); final yield 1.5 g (30%) with GC purity of 99.15%. ^{1}H NMR ($CDCl_3$, 500 MHz) δ (ppm): 2.353–2.397 (m, 2*H*), 2.725 (t, 2*H*), 4.974–5.057 (m, 2*H*), 5.797–5.878 (m, 1*H*), 7.167–7.199 (m, 4*H*), 7.428–7.444 (d, J = 8 Hz, 2*H*), 7.470–7.496 (m, 2*H*); IR (KBr, cm^{-1}): 3079, 3027, 2979, 2853, 2187, 2095 (NCS, *v*), 1594, 1514, 1429, 1204, 1101, 933, 834; MS *m*/*z* (RI, %): 289.1 (M^+, 100), 248.0 (64), 189.1 (29), 215.1 (59).

A2: The same procedure as **A1**; an amount of 2.8 g compound **A2** was obtained with yield of 31% and purity of 99.25% (GC). ^{1}H NMR ($CDCl_3$, 500 MHz) δ (ppm): 2.354–2.399 (m, 2*H*), 2.730 (t, J = 6.5 Hz, 2*H*), 4.976–5.058 (m, 2*H*), 5.795–5.876 (m, 1*H*), 7.120–7.190 (m, 3*H*), 7.236–7.296 (m, 2*H*), 7.424–7.441 (d, J = 8.5 Hz, 2*H*); IR (KBr, cm^{-1}): 3076, 3026, 2976, 2852, 2208, 2044 (NCS, *v*), 1557, 1515, 1422, 1209, 1104, 960, 870; MS *m*/*z* (RI, %): 307.3 (M^+, 100), 233.2 (82), 266.2 (61), 207.2 (46).

A3: The same procedure as **A1**; an amount of 1.7 g compound **A3** was obtained with yield of 26% and purity of 99.06% (GC). ^{1}H NMR ($CDCl_3$, 500 MHz) δ (ppm): 2.354–2.398 (m, 2*H*), 2.729 (t, J = 15.5 Hz, 2*H*), 4.975–5.053 (m, 2*H*), 5.795–5.876 (m, 1*H*), 6.955–7.010 (m, 2*H*), 7.174–7.190 (d, J = 8Hz, 2*H*), 7.449–7.481 (m, 3*H*); IR (KBr, cm^{-1}): 3074, 3024, 2977, 2925, 2219, 2114 (NCS, *v*), 1555, 1515 (Ar, *v*), 1422, 1235, 1105, 910, 868, 819; MS *m*/*z* (RI, %): 307.6 (M^+, 100), 266.4 (59), 207.5 (49).

A4: The same procedure as **A1**; an amount of 3.0 g compound **A4** was obtained with yield of 35% and purity of 99.19% (GC). ^{1}H NMR($CDCl_3$, 500 MHz) δ (ppm): 2.355–2.395 (m, 2*H*), 2.732 (t, J = 15.5 Hz, 2*H*), 4.980–5.054 (m, 2*H*), 5.793–5.874 (m, 1*H*), 7.074–7.110 (m, 2*H*), 7.179–7.195 (d, J = 8 Hz, 2*H*), 7.419–7.435 (d, J = 8 Hz, 2*H*); IR (KBr, cm^{-1}): 3066, 3024, 2974, 2862, 2200, 2077 (NCS, *v*), 1565, 1512, 1430, 1203, 1101, 1040, 927, 911, 854, 819; MS *m*/*z* (RI, %): 325.8 (M^+, 100), 284.5 (58), 225.6 (50), 207.6 (15).

3. Results and discussion

3.1. The effect of terminal chain on mesophase properties

Table 1 lists the phase transition temperatures and associated enthalpy changes of four new isothiocyanatotolanes with but-3-enyl as terminal group and their comparison structures with *n*-butyl as terminal group.

As for the isothiocyanatotolanes with single fluoro substitute in site Z, replacing *n*-butyl chain by but-3-enyl as terminal group reveals a decrease of melting point about 10°C and a half decrease of the melting enthalpy value. As for the isothiocyanatotolanes with fluoro substitute in site X, replacing *n*-butyl chain by but-3-enyl as terminal group displays an obvious decrease of the melting enthalpy value. Moreover, the

Table 1. Phase transition temperatures and associated enthalpy of the compounds **A1–B4** from DSC measurements.

	Phase transition temperatures (°C) (enthalpy change (kJ/mol)	
Compound	Heating process	Cooling process
AA1	Cr 79.84 (17.27) I	I 72.71 (17.90) Cr
AA2	Cr 46.54 (16.94) I	I 34.37 (0.24) N 27.13 (15.37) Cr
AA3	Cr 48.73 (16.85) I	I 51.80 (0.38) N 36.78 (14.21) Cr
AA4	Cr 50.57 (25.44) I	I 25.60 (17.23) Cr
BB1	Cr 48.31(0.10) SmK 72.74 (0.84) SmE 86.72 (12.84) I	I 86.31 (12.98) SmK 69.44 (0.91) Cr
BB2	Cr 39.69 (23.54) I	I 18.02 (0.19) N 11.67 (14.52) Cr
BB3	Cr 58.80 (32.98) I	I 29.80 (0.30) N 11.89 (24.48) Cr
BB4	Cr 31.62 (25.03) I	I < 20 Cr

Cr: Crystal; S: smectic phase; N: nematic phase; I: isotropic liquid.

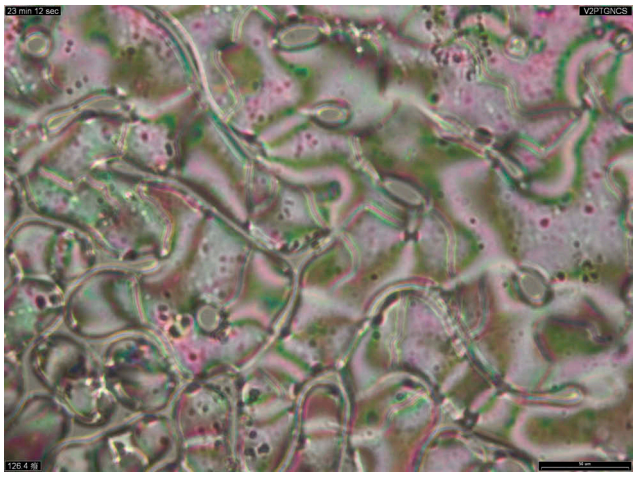

Figure 2. (colour online) Photo micrographs (×200), Nematic schlieren texture of **A2** when cooled to 26.4°C.

compounds with single fluorine (**A2** and **A3**) exhibit much higher clearing points in cooling process than those of the reference compounds.

The textures of the new compounds were examined with POM. The observed phase transitions were identical with those from DSC curves. The POM micrographs of compound **A2** are given in Figure 2.

3.2. The effect of lateral fluorine substitution on mesophase properties

From Figure 3, the compound without lateral fluorine (**A1**) exhibits a relatively high melting point of 79.84°C. After introduction of lateral fluoro atom into the X or Z position, the melting points fall down to 46.54°C and 48.73°C, respectively. Comparing compounds **A2** with **A3**, we find that the compound with fluorine in the X position has lower melting point than that of the compound with the fluorine in the Z position. After introduction of lateral difluorine substitutes into the X and Y position, the melting point increased slightly to 50.57°C.

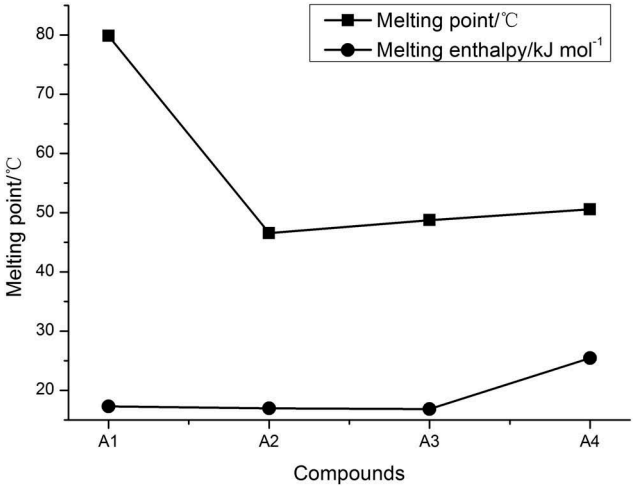

Figure 3. The effect of lateral fluorine substitute on mesophase properties.

Table 2. Calculated and measured birefringence of the investigated compounds, and their extrapolated rotational viscosity.

Compound	$\bar{\alpha}$ (au)	$\Delta\alpha$ (au)	Δn_{calc}	Δn_{extra}	γ_{1extra} (mPa s)
A1	256.22	418.18	0.444	0.430	35.17
A2	260.18	429.74	0.429	0.422	30.98
A3	259.37	422.77	0.422	0.418	20.48
A4	263.95	428.58	0.404	0.394	21.29
B1	253.26	403.95	0.426	0.406	41.35
B2	257.22	415.45	0.412	0.400	38.44
B3	256.42	408.52	0.405	0.405	21.79
B4	261.00	414.32	0.388	0.364	23.19

Compounds **A1, A2** and **A3** exhibit closely melting enthalpy value of about 17 kJ/mol, while compound **A4** exhibits slightly high melting enthalpy value of 25 kJ/mol.

As shown in Table 1, the compound without fluorine (**A1**) and the compound with lateral difluorine (**A4**) do not exhibit nematic phase, while single fluoro-substituted compounds **A2** and **A3** exhibit monotropic nematic phase range about of 7 and 15°C.

3.3. Physical properties

In order to investigate the properties of single compound, 10 wt% of the guest compound was dissolved in a room temperature LC host mixture P0.

By knowing the birefringence of the host mixture, the Δn of the guest compound at room temperature can be estimated according to the following equation [22]:

$$(\Delta n)gh = x(\Delta n)g + (1-x)(\Delta n)h \qquad (1)$$

where gh, g and h are the birefringence of the guest–host system, guest compound and host mixture, respectively. The Δn value of the target compounds and their comparison structures, and the rotation viscosity value were ex trapolated and listed in Table 2.

As shown in Table 2, compound **A1** has the largest Δn value of about 0.43. Further fluorination in the position of X, Y and Z shows an effect of dropping the Δn value of about 0.002–0.036. The compound with

Table 3. Test mixtures **A** and **B** and their properties.

Mix	Composition	γ_1 (mPa s)	K_{11} (pN)	Nematic temperature range (°C)
Mix **A**	Host + 15 wt% **A1** + 5 wt% **A2**	155	12.5	−5–106.6
Mix **B**	Host + 15 wt% **B1** + 5 wt% **B2**	180	11.0	0–105.8

fluorine in the X position (**A2**) has a little higher Δn than that of the corresponding compounds with fluorine in the Z position (**A3**). The compound with difluorine in the X and Y positions (**A4**) has the lowest Δn value of 0.394. Series A exhibits higher Δn values between 0.394 and 0.430 than those of the reference series **B** because of the larger π-electron conjugation. Series **A** exhibits lower rotational viscosity in 20.48–35.17 mPa s than that of the *n*-butyl analogues **B**.

We carried out the theoretical calculation of the Δn values and the results are given in Table 2. The values of average polarisability ($\bar{\alpha}$) and polarisability anisotropy ($\Delta\alpha$) were calculated from α_{xx}, α_{yy} and α_{zz} that come from the semi-empirical AM1 method acting on the relevant chemical structure. The Δn values were enumerated using the Vuks formula [23], while the density and the order parameter S were assumed to be 1.0 g/cm^3 and 0.60, respectively. The calculated Δn values (Δn_{calc}) are very close to their experimental data (Δn_{extra}), and series **A** have larger polarisability anisotropy ($\Delta\alpha$) than that of series **B**. According to the Vuks formula, birefringence is proportional to polarisability anisotropy, which can explain why series **A** have higher birefringence.

3.4. High birefringence mixtures

Based on the results of single component, we formulated two different high birefringence test mixtures **A** and **B** which composed of the same host mixture and doped single compound, and the mixtures **A** and **B** and their some physical properties at 21°C are presented in Table 3.

The physical properties of mixtures **A** and **B** were measured by using the experimental setup and measurement technique reported in [24]. They were filled into a homogeneous cell of cell gap d – 5 μm. Birefringence can be obtained by measuring the voltage-dependent transmittance (VT) of a homogeneous cell sandwiched between two crossed polarisers. A linearly polarised He–Ne laser (λ = 633 nm) was used as light sources. The corresponding VT curves and phase retardation were measured. The birefringence at a given wavelength and temperature was obtained from the phase retardation based on the following equation [25]:

$$\delta = \frac{2\pi d\Delta n}{\lambda} \tag{2}$$

The temperature-dependent birefringence was measured from 21 to 75°C, and the results for λ = 633 nm are plotted in Figure 4, where dots are experimental data and solid line is the fitting curve based on Haller's semi-empirical equation [26].

$$\Delta n = \Delta n_0 \left(\frac{1-T}{Tc}\right)^{\beta} \tag{3}$$

where Δn_0 is the extrapolated birefringence at T = 0 K and β is a material constant. Through fitting, for Mix **A**, we find Δn_0 = 0.565 and β = 0.233, and for Mix **B**, we find Δn_0 = 0.555 and β = 0.226. As the temperature

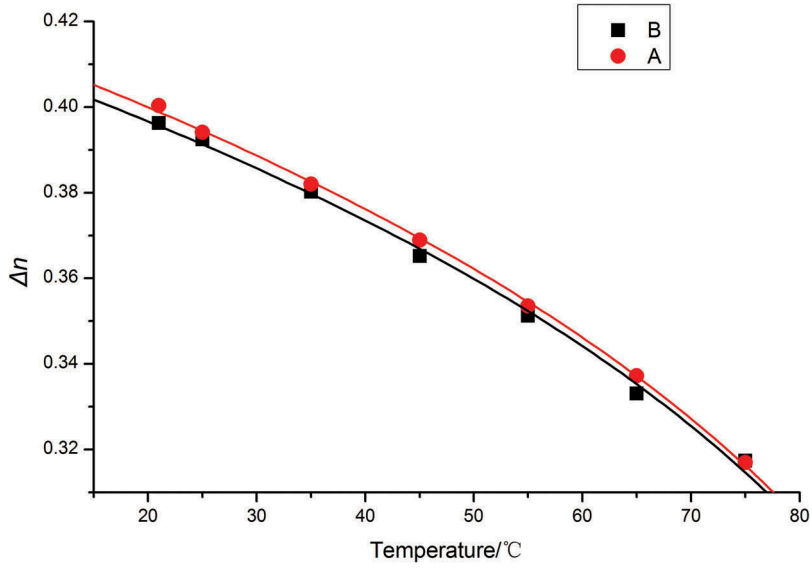

Figure 4. (colour online) Temperature-dependent birefringence of mixtures **A** and **B** at λ = 633 nm: dots stand for measured data and solid line for fitting curve with Equation (3).

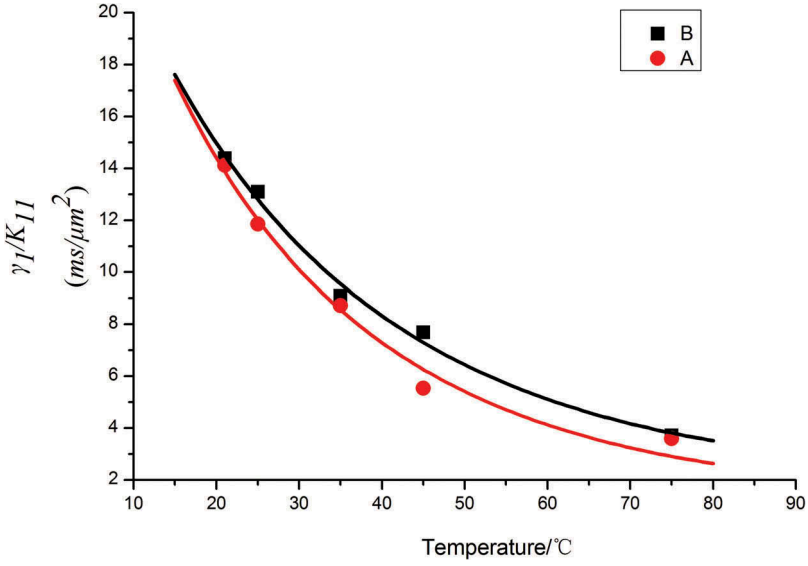

Figure 5. (colour online) Temperature-dependent visco-elastic coefficient of mixes **A** and **B**: dots are measured data and solid lines are fitting with Equation (5). λ = 633 nm.

increases, the value of birefringence of Mix **A** is higher than that of Mix **B**.

The visco-elastic coefficient (γ_1/K_{11}) was obtained by measuring the dynamic free relaxation time for a controlled phase change as [26]:

$$\tau_0 = \frac{\gamma_1 d^2}{k_{11}\pi} \tag{4}$$

where τ_0 is the relaxation time, γ_1 is rotational viscosity and K_{11} is the splay elastic constant. We plot visco-elastic coefficient for Mixtures **A** and **B** at different temperatures in Figure 5, where dots are experimental data and solid lines are fitting curve with following equation [27]:

$$\frac{\gamma_1}{k_{11}} = A\frac{\exp(E/K_B T)}{(1 - T/T_c)^{\beta}} \tag{5}$$

In Equation (5), A is a proportional constant, E is the activation energy, T is the Kelvin temperature and K_B is the Boltzmann constant. For Mix **A**, we find $A = 9.02 \times 10^{-5}$ ms/μm^2 and E = 282 meV. For Mix **B**, we find $A = 4.27 \times 10^{-4}$ ms/μm^2 and E = 246 meV. Mix **A** has a smaller visco-elastic coefficient (~11.8 ms/μm^2) than Mix **B** (~13.1 ms/μm^2) at room temperature. As the temperature increases, the visco-elastic coefficient of Mix **A** decreases more significantly than Mix **B**.

We plot FoM for mixtures **A** and **B** at different temperatures in Figure 6, where dots are experimental data and solid lines are fitting curve with following equation [24]:

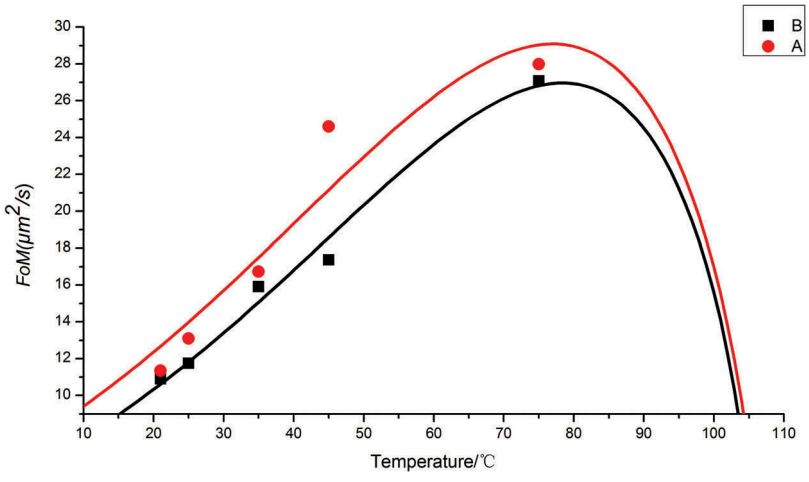

Figure 6. (colour online) Temperature-dependent FoM of mixtures **A** and **B**: dots are measured data and solid lines are fitting with Equation (6). λ = 633 nm.

$$\mathrm{FoM} = \alpha(\Delta n^2)\left(1 - \frac{T}{T_c}\right)^{3\beta} \exp\left(\frac{-E}{K_B T}\right) \qquad (6)$$

where α is a fitting parameter, T_c is clearing point temperature. Mix **A** shows a clearing point temperature of 106.6°C, and Mix **B** shows of 105.8°C.

In Figure 6, Mix **A** shows the highest FoM which is 29 μm^2/ms at 70–80°C, while Mix **B** shows the highest FoM which is 27 μm^2/ms at 70–80°C. As the temperature increases, Figure 6 shows that Mix **A** has higher FoM than Mix **B**. The low T_c of Mix **B** negatively affects its birefringence and, moreover, its visco-elastic coefficient is relatively high, as a result, its FoM is low. That is a consequence of longer π-electron conjugation and lower rotational viscosity of the but-3-enyl chain in comparison to saturated *n*-butyl chain.

4. Conclusions

We have developed a series of new but-3-enyl-based isothiocyanatetolane substances and evaluated their mesomorphic and electro-optical properties. As expected, replacing saturated *n*-butyl chain by but-3-enyl chain not only increases the values of Δn but also decreases the rotational viscosity of the compounds. When compounds **A1** and **A2** and **B1** and **B2** were used in test mixture, the mixture-based **A1** and **A2** exhibits broader nematic phase temperature range, higher birefringence, lower visco-elastic coefficient and higher value of FoM, which makes them suitable dopants for high birefringence systems.

Disclosure statement

No potential conflict of interest was reported by the authors.

Funding

This work was supported by the Defense Industrial Technology Development Program of China [Grant Numbers: B1120132028]; The State Key Laboratory of Applied Optics [Grant Numbers: Y6133FQ112].

References

[1] Jesacher A, Maurer C, Schwaighofer A, et al. Near-perfect hologram reconstruction with a spatial light modulator. Opt Express. 2008;16:2597–2603. DOI:10.1364/OE.16.002597
[2] Khan SA, Riza NA. Demonstration of 3-dimensional wide angle laser beam scanner using liquid-crystals. Opt Express. 2004;12:868–882. DOI:10.1364/OPEX.12.000868
[3] Grudniewski T, Parka J, Dabrowski R, et al. Photo refractive effects in pure multicomponent isothiocyanate liquid crystals under low power illumination. Mol Cryst Liq Cryst. 2004;413:443–450. DOI:10.1080/15421400490439086
[4] Ren HW, Fan YH, Gauza S, et al. Tunable-focus flat liquid crystal spherical lens. Appl Phys Lett. 2004;84:4789–4791. DOI:10.1063/1.1760226
[5] Pishnyak O, Sato S, Lavrentovich OD. Electrically tunable lens based on a dual-frequency nematic liquid crystal. Appl Opt. 2006;45:4576–4582. DOI:10.1364/AO.45.004576
[6] Reuter M, Garbat K, Vieweg N, et al. Terahertz and optical properties of nematic mixtures composed of liquid crystal isothiocyanates, fluorides and cyanides. J Mater Chem C. 2013;1:4457–4463. DOI:10.1039/c3tc30464g
[7] Scherger B, Reuter M, Scheller M, et al. Discrete Terahertz beam steering with an electrically controlled liquid crystal device. J Infrared Millim Terahertz Waves. 2012;33:1117–1122. DOI:10.1007/s10762-012-9927-5
[8] Spadło A, Dabrowski R, Filipowicz M, et al. Synthesis, mesomorphic and optical properties of isothiocyanatotolanes. Liq Cryst. 2003;30:191–198. DOI:10.1080/0267829021000060197
[9] Dabrowski R. Isothiocyanates and their mixtures with a broad range of nematic phase. Mol Cryst Liq Cryst. 1990;191:17–27.
[10] Wen CH. High birefringence and low viscosity liquid crystals[D]. Orlando (PA): University of Central Florida; 2006.
[11] Gauza S, Wu ST, Spadlo A, et al. High performance room temperature nematic liquid crystals based on laterally fluorinated isothiocyanato-tolanes. J Disp Technol. 2006;2:247–253. DOI:10.1109/JDT.2006.878770
[12] Catanescu CO, Chien LC, Wu ST. High birefringence nematic liquid crystals for display and telecom applications. Mol Cryst Liq Cryst. 2004;411:93/[1135]–102/[1144]. DOI:10.1080/15421400490434829
[13] Gauza S, Wen CH, Wu B, et al. High figure-of-merit nematic mixtures based on totally unsaturated isothiocyanate liquid crystals. Liq Cryst. 2006;33:705–710. DOI:10.1080/02678290600703916
[14] Dabrowski R. New liquid crystalline materials for photonic applications. Mol Cryst Liq Cryst. 2004;421:1–21. DOI:10.1080/15421400490501112
[15] Peng ZH, Wang QD, Liu YG, et al. Electrooptical properties of new type fluorinated phenyl-tolane isothiocyanate liquid crystal compounds. Liq Cryst. 2015;1:1–8.
[16] Catanescu CO, Wu ST, Chien LC. Tailoring the physical properties of some high birefringence isothiocyanato-based liquid crystals. Liq Cryst. 2004;31:541–555. DOI:10.1080/02678290410001662240.
[17] Schadt M, Buchecker R, Villiger A. Synergisms, structure-material relations and display performance of novel fluorinated alkenyl liquid crystals. Liq Cryst. 1990;7:519–536. DOI:10.1080/02678299008033829.
[18] Kelly SM. The effect of the position and configuration of carbon-carbon double bonds on the mesomorphism of thermotropic, non-amphiphilic liquid crystals. Liq Cryst. 1996;20:493–515. DOI:10.1080/02678299608031137.
[19] Kirsch P, Heckmeier M, Tarumi K. Design and synthesis of nematic liquid crystals with negative dielectric anisotropy. Liq Cryst. 1999;26:449–452. DOI:10.1080/026782999205236.
[20] Jiang Y, An ZW, Chen P, et al. Synthesis and mesomorphic properties of but-3-enyl-based fluorinated biphenyl liquid crystals. Liq Cryst. 2012;39:457–465.

[21] Li J, Hu MG, Li JL, et al. Highly fluorinated liquid crystals with wide nematic phase interval and good solubility. Liq Cryst. 2014;41:1783–1790. DOI:10.1080/02678292.2014.950617.
[22] Gauza S, Parish A, Wu ST, et al. Physical properties of laterally fluorinated isothiocyanato phenyl-tolane single liquid crystals components and mixtures. Mol Cryst Liq Cryst. 2008;489:135–147. DOI:10.1080/15421400802219759.
[23] Vuks MF. Determination of optical anisotropy of aromatic molecules from double refraction of crystals. Opt Spectrosc. 1966;20:361–368.
[24] Wu ST, Efron U, Hess LD. Birefringence measurementsof liquid crystals. Appl Opt. 1984;23:3911–3915. DOI:10.1364/AO.23.003911.
[25] Haller I. Thermodynamic and static properties ofliquid crystals. Prog Solid State Chem. 1975;10:103–118. DOI:10.1016/0079-6786(75)90008-4.
[26] Wu ST, Wu CS. Experimental confirmation of the Osipov–Terentjev theory on the viscosity of nematic liquid crystals. Phys Rev A. 1990;42:2219–2227. DOI:10.1103/PhysRevA.42.2219.
[27] Peng FL, Chen Y, Wu ST, et al. Low loss liquid crystals for infrared applications. Liq Cryst. 2014;1:1–8.